Differential and Integral Cross Sections for the Excitation of the $2\,^1S$, $2\,^3S$, and $2\,^3P$ States of He by Electron Impact at 29.6 and 40.1 eV

S. Trajmar*

Jet Propulsion Laboratory, California Institute of Technology, Pasadena, California 91103

(Received 12 February 1973)

Differential and integral cross sections for the electron-impact excitation of the $2\,^3S$, $2\,^1S$, and $2\,^3P$ states of He relative to the $2\,^1P$ state have been measured at 29.6- and 40.1-eV energies in the 3° to 138° angular range. The relative cross sections have been normalized to the absolute scale by utilizing the previously determined $2\,^1P$ cross sections [D. G. Truhlar, S. Trajmar, W. Williams, S. Ormonde, and B. Torres (unpublished)]. The differential cross section for the $2\,^1S$ state has a deep minimum at 50°; for the $2\,^3P$ state it is nearly isotropic, and for the $2\,^3S$ state it shows a complicated structure which has not been previously reported. The experimental cross sections are compared to the results of quantum-mechanical calculations performed by Truhlar, Yates, Tenney, Cartwright, Steelhammer, and Lipsky using the Born, Born-Ochkur-Rudge, and Glauber approximations for the $2\,^1S$ excitation and the Born-Oppenheimer and the Ochkur-Rudge approximations for the $2\,^3S$ and the $2\,^3P$ excitations. None of the first-order plane-wave calculations predict the observed differential cross sections for these optically forbidden transitions. It is interesting to note, however, that the Ochkur-Rudge model predicts the correct magnitude and approximate shape of the $2\,^3P$ differential cross sections in the whole angular range at these energies. The Glauber approximation shows considerable improvement compared to first-order plane-wave theories in predicting the cross sections for the $2\,^1S$ state. However, at large scattering angles, calculation and experiment differ significantly. It is clear from the present study that more refined calculations are needed to predict angular distributions for these optically forbidden excitations in the 30–40-eV energy region.

I. INTRODUCTION

Electron-impact excitation of He at intermediate energies ($E_0 \approx 25$–100 eV) is of considerable interest not only for its practical importance but also from the theoretical point of view. At near-threshold regions, resonance theories and close-coupling calculations yield quite reliable predictions. At high impact energies, the Born (B) and other first-order approximations are applicable, and at very high impact energies the excitation processes are governed by optical selection rules. The most difficult region for theoretical attack is the intermediate-energy region.

Elastic scattering and the excitation of the $2\,^1P$ state of He by electron impact have been widely studied both experimentally and theoretically. The measurements have served as a testing ground for various models and approximations and considerable success has been achieved.[1–5] The same cannot be said for the optically forbidden $2\,^1S$ excitation and for the $2\,^3S$ and $2\,^3P$ spin-exchange excitation processes. Although several measurements and calculations have been reported on the integral cross sections Q, only a very limited amount of experimental and theoretical work has been done on the differential cross sections (DCS) for these excitation processes.

A comprehensive survey of the early work dealing with the excitation of the $n=2$ manifold states has been given by Massey and Burhop.[1] Relative differential cross sections for the excitation of these states were determined by a number of investigators.[6–13] By combining the relative measurements of Refs. 9–11 and 13 with the normalized $2\,^1P$ cross sections[2] one can obtain normalized cross sections at 26.5, 34, 44, 55.5, and 81.6 eV. Opal and Beaty[14] studied these processes at 82 eV in the 30°–150° angular range with low energy-resolution. A large number of measurements were carried out by Crooks[15] in the 10°–150° angular range (at 50 and 100 eV). Very recently Hall *et al.*[16] obtained cross sections for these excitation processes in the 10°–125° angular range (at 29.2, 39.2, and 48.2 eV). The differential cross sections for the excitation of the $2\,^3S$ state were measured by Crooks *et al.*[17] from 40 to 70 eV at angles ranging from 25° to 150°. (Work carried out near threshold or at impact energies above 100 eV are not discussed here.)

The excitation of the $2\,^1S$ state has been considered theoretically in detail by Rice *et al.*[13] and by Yates and Tenney.[18] Rice *et al.* reported experimental cross sections and calculations based on first-order and polarization scattering models. It was concluded that in order to properly describe scattering at low angles it was necessary to include the polarization effects in the generalized optical potential. None of the plane-wave theories considered could predict the differential cross

sections at high scattering angles. The only absolute measurement for the $2\,^1S$ excitation was carried out by Chamberlain *et al.*[19] at 5°, at several energies ranging from 50 to 150 eV. Hidalgo and Geltman[20] studied the $2\,^1S$ excitation by the Coulomb-projected Born approximation, at and above impact energies of 100 eV, and found that the interaction of the scattered electron with the nucleus significantly influenced the values of the calculated cross sections. Yates and Tenney[18] applied the Glauber (G) approximation at intermediate energies and found good agreement up to an 80° scattering angle with the available experimental data at 26.5, 34, 50, and 82 eV. In the Glauber model polarization and distortion are taken into account in an approximate way, but exchange is neglected. Kohl *et al.*[21] used the eikonal approximation to obtain the excitation cross section for the $2\,^1S$ state from 0° to 20° angular range at energies of 50–500 eV. They found that this method gave improved results with respect to first-order Born calculations, but the calculated angular dependence was in disagreement with the experimental results.

Differential cross sections for the excitation of the $2\,^3S$ and $2\,^3P$ states were calculated by Cartwright[22] and by Steelhammer[23] in the framework of the Ochkur-Rudge (OR) and Born-Opperheimer (BO) approximations. The OR approximation was found to give the correct magnitude for the integral cross sections, but predicted DCS peaking at intermediate angles. Experimental measurements show forward peaking for the $2\,^3S$[7,11,24] and nearly isotropic distributions for the $2\,^3P$ excitations.[11] The BO approximation predicted forward peaking for the $2\,^3S$ DCS but disagreed with the experimental angular distribution at high angles. Furthermore, the values of the calculated cross sections were considerably higher than the experimental[11] ones. Better agreement in magnitude was found for this approximation for the $2\,^3P$ excitation, but the calculated angular distribution disagreed with experiments at large scattering angles.[11]

II. EXPERIMENTAL

The apparatus utilized to carry out the measurements has been described elsewhere.[25] A He atomic beam was crossed by an energy-selected electron beam and the scattering intensity as a function of energy loss, at fixed scattering angles θ ranging from 3° to 138°, was measured for the excitation of the $n=2$ manifold at 29.6 and 40.1 eV impact energies E_0. Each energy-loss spectrum was obtained by the superposition of 5–200 scans, utilizing a multichannel scaler, until adequate signal-to-noise conditions were achieved, even for the weakest feature in the spectrum. Typical spectra are shown in Fig. 1.

The symmetry of the scattering around 0° was confirmed from −15° to +15°. The acceptance solid angle extended by the detector aperture at the scattering center was 6.8×10^{-4} sr. The view cone for the detector was defined by two circular apertures and the cone half-angle was 1.6°. In general, the angular resolution cannot be easily defined or experimentally determined. The detector accepts scattered signals from all points within the view cone and therefore the extreme angular resolution could be taken as equal to the view cone angle. In actual practice the angular resolution is better than this value. The reason

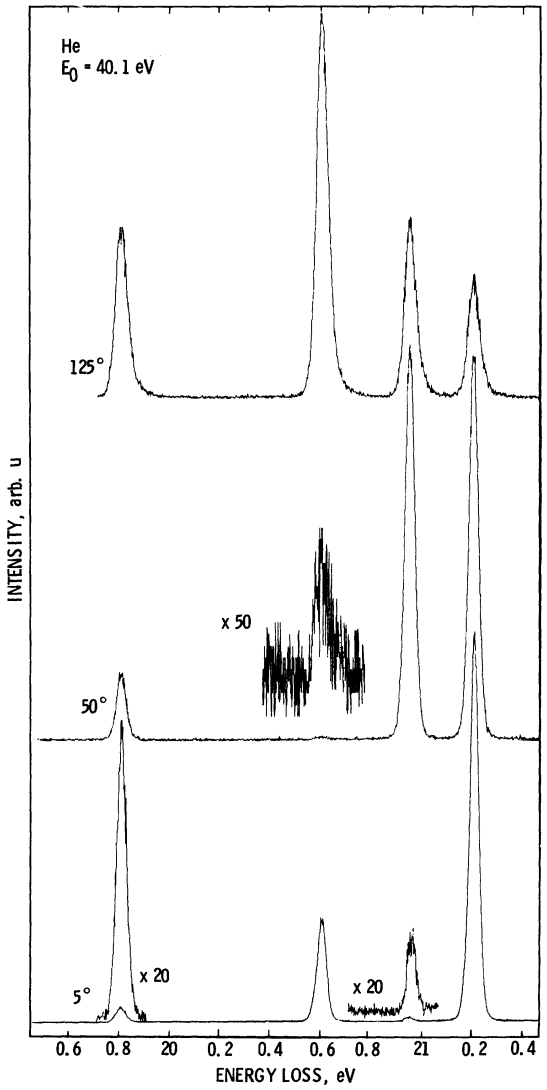

FIG. 1. Typical energy-loss spectra at 40.1-eV impact energy and at scattering angles of 5°, 50°, and 125°.

is that the array of scattering points have different angular ranges associated with them over which the signal is seen and integrated by the detector. In other words, in the total signal a weighing factor can be assigned to each scattering angle that contributes to the detected signal. One could then take the full width at half-maximum of this weighted distribution versus θ as the angular resolution. It is not practical to determine the angular resolution in this manner, however, since it will change with nominal scattering angle and with scattering geometry. To determine the angular resolution experimentally, it would be necessary to have a feature in an angular distribution whose width is known to be less than the angular resolution of the instrument. The deep minimum in the $2\,^1S$ DCS may be such an appropriate feature. The presently measured angular distribution has a deeper minimum than the ones measured previously with instruments known to have poorer angular resolutions. It will be required to remeasure this distribution with an even higher angular resolution to see whether the present shape was predominantly determined by the instrument or by the actual behavior of the differential cross section. At the present time we can only state that on the basis of extreme geometrical considerations, the angular resolution is between 1.7° and 3.2°. This angular resolution is sufficient to bring out certain features in the angular distributions that were not previously observed.

The calibration of the impact-energy scale is discussed elsewhere.[5]

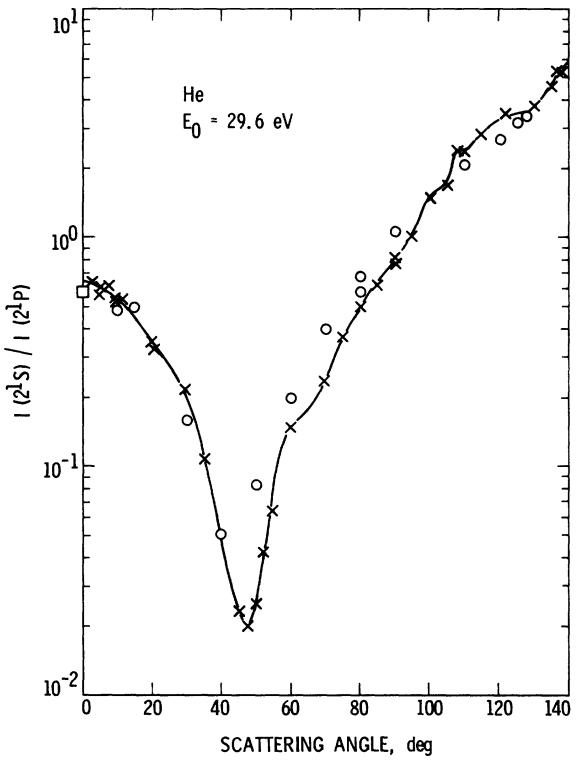

FIG. 2. Ratio of the scattering intensity of the $1\,^1S \rightarrow 2\,^1S$ transition to that of the $1\,^1S \rightarrow 2\,^1P$ transition as a function of scattering angle. The present experimental points at 29.6 eV (crosses) are joined by a smooth curve. The values measured by Hall *et al.* (Ref. 12) at 29.2 eV (circles) are given for comparison.

III. CROSS-SECTION RATIOS

The most accurately determined quantities in the present measurements are the scattering intensity ratios within the $n=2$ manifold. The electron optics were designed to be independent of the value of energy loss. Furthermore, drifts are averaged out and statistical errors are reduced to below a few percent by the superposition of many scans, and all angular-dependent errors cancel out in the ratios. In general, the ratios are estimated to be accurate to within 5%.

The ratios were obtained by measuring the heights of the individual peaks above the background. This is a well-justified procedure under the present experimental conditions, as verified by integrating the area under the peaks for a few specific cases. Figures 2–7 give the measured intensity ratios with respect to the $2\,^1P$ intensities. The intensity ratios measured by Hall *et al.*[12] are also given.

The $2\,^3S$ ratio curves show complicated structures and are significantly different at the two impact energies. These structures are reported for the first time and are believed to be real, since they are larger than the estimated error

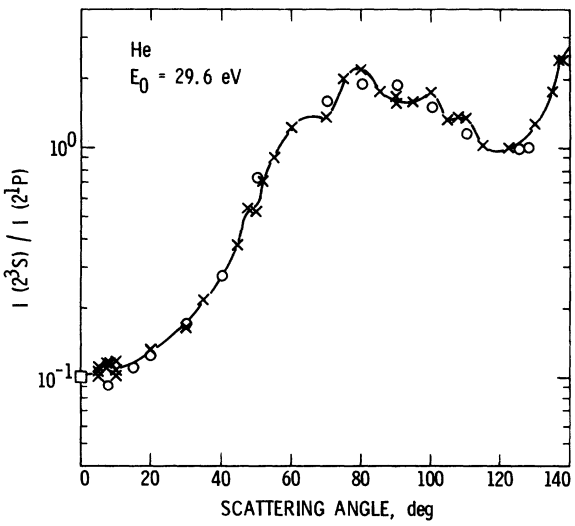

FIG. 3. Same as Fig. 2, except this is for the $1\,^1S \rightarrow 2\,^3S$ transition.

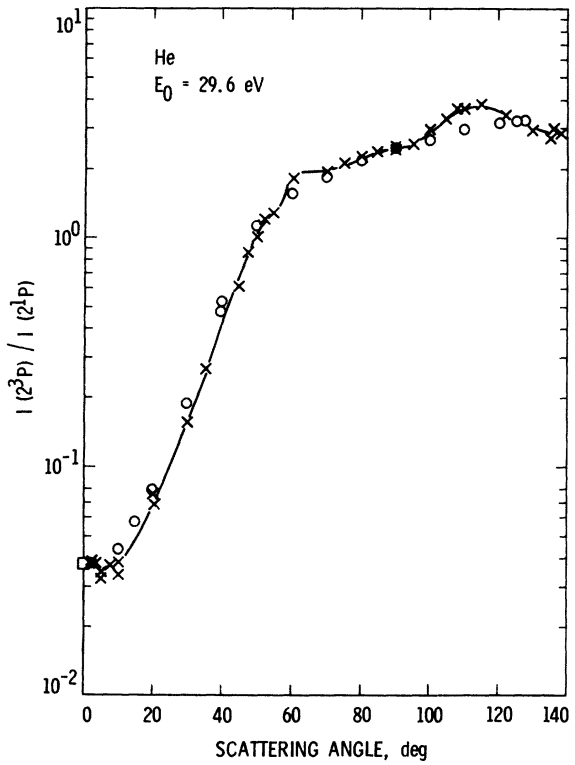

FIG. 4. Same as Fig. 2, except this is for the $1^1S \rightarrow 2^3P$ transition.

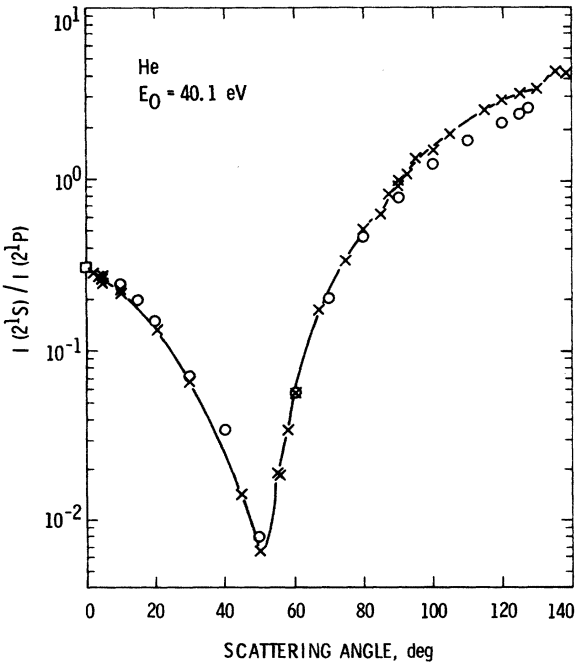

FIG. 5. Same as Fig. 2, except the present values (crosses) are at 40.1-eV impact energy, and those of Hall *et al.* (Ref. 12) are at 39.2-eV impact energy (circles).

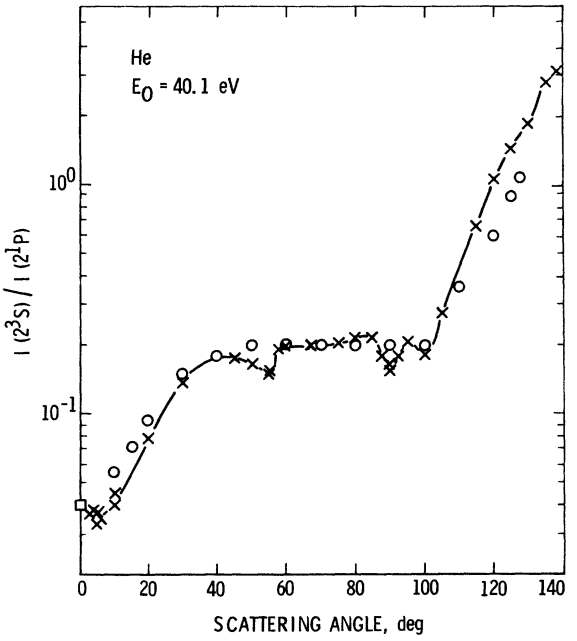

FIG. 6. Same as Fig. 5, except this is for the $1^1S \rightarrow 2^3S$ transition.

limits. The 2^1S and 2^3P ratio curves remained qualitatively the same at the two impact energies. There seems to be an indication for a slight minimum in the 2^3P ratio curves at around 5° at both energies.

IV. DIFFERENTIAL CROSS SECTIONS

From the intensity ratios and from the previously determined 2^1P cross sections,[5] the DCS

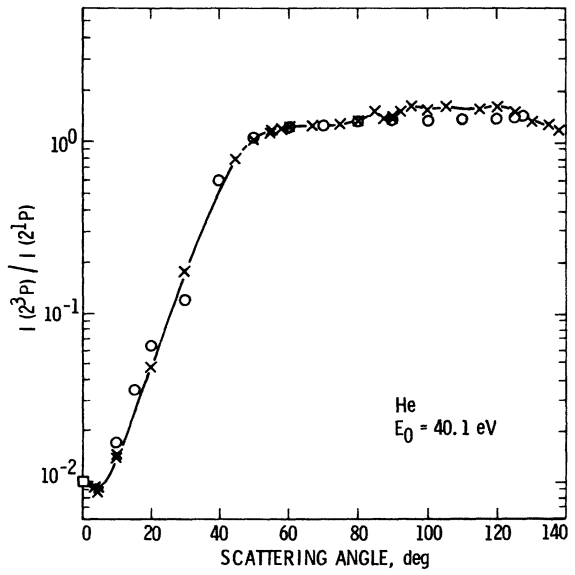

FIG. 7. Same as Fig. 5, except this is for the $1^1S \rightarrow 2^3P$ transition.

for the other $n=2$ manifold excitations were obtained. The results are summarized in Figs. 8–13. The intensity ratios are given in Table I and the differential cross sections are given in Tables II–IV for convenience and for the purpose of possible recalculation of the cross sections when more accurate $2\,^1P$ cross sections become available.

The present results are compared in Figs. 8–13 with the very recent measurements of Hall *et al.*[16] The latter measurements were carried out with a different type of apparatus and have been normalized to the absolute scale by a completely different method. They calibrated the over-all instrument efficiency by measuring the scattering intensities of the $n=2$ manifold excitations and the He elastic scattering intensities corresponding to an impact energy equal to the residual energy of the inelastically scattered electrons and then utilizing the known absolute electron-He elastic cross sections.[26] Their results are in excellent over-all agreement with the present measurements. There are, however, some differences in the finer details of the curves. These differences may be attributed to the fact that the present results were obtained with better angular resolution. The $2\,^3S$ DCS measured by Crooks *et al.*[17] at 40 eV are also shown in Fig. 12. They utilized a third type of instrument and achieved the normalization to the absolute scale by directly determining all the quantities that relate the measured scattering intensities to the respective cross sections. The agreement among the different measurements is excellent. Also shown in Figs. 8–13 and given in Tables II–IV are the calculated cross sections using the B, the Born-Ochkur-Rudge (BOR), and the G approximations for the $2\,^1S$ state and the BO and the OR approximations for the $2\,^3S$ and $2\,^3P$ states.

The calculations[27] for excitation of the $2\,^1S$ state using the B[28] and BOR[2,29,30] approximations were performed by methods described previously.[13,31] These calculations used the generalized oscillator strengths obtained from very accurate wave functions[32] by Kim and Inokuti.[33] The calculations[34] using the G approximation were performed as described in Ref. 18. The calculations[22,35] for excitation of the $2\,^3S$ state using the BO[36,37] and OR[38] approximations were performed as described in Refs. 22 and 23. These calculations used the wave

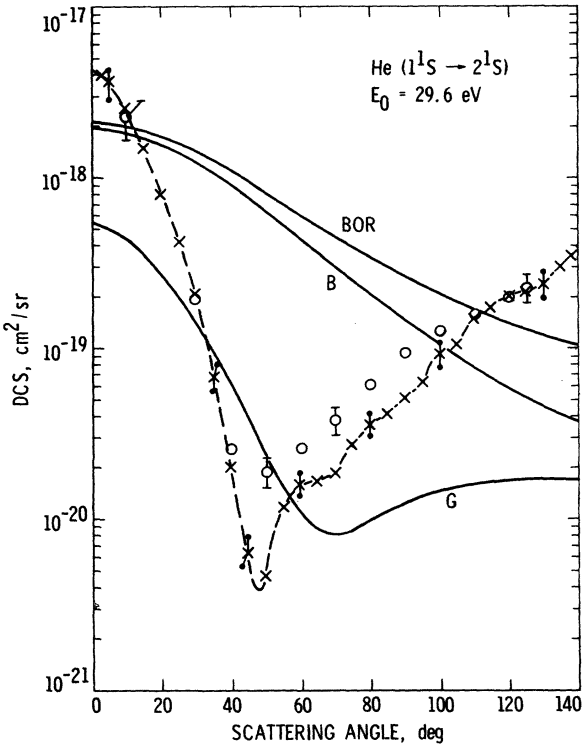

FIG. 8. Differential cross sections for the excitation of the $2\,^1S$ state. The present experimental points at 29.6 eV (crosses) are joined by the dash-dash curve. The values measured by Hall *et al.* (Ref. 16) at 29.2 eV (circles) are given for comparison. Representative error bars are shown. The solid curves are the results of calculations utilizing the Born (B), Born-Ochkur-Rudge (BOR) (Ref. 27), and Glauber (G) (Ref. 34) approximations at 30, 30, and 29.6 eV, respectively.

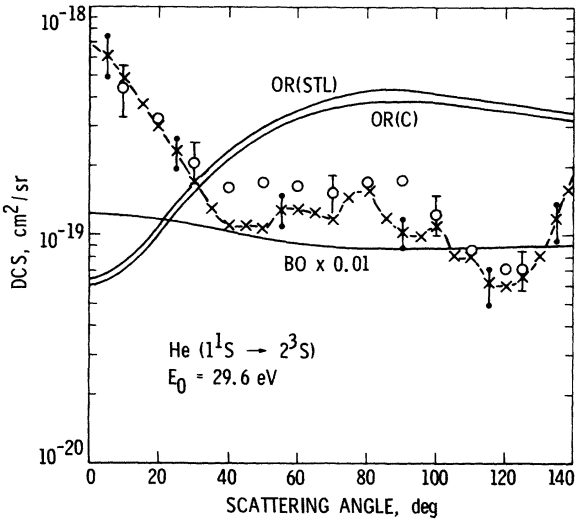

FIG. 9. Differential cross sections for the excitation of the $2\,^3S$ state. The present experimental points at 29.6 eV (crosses) are joined by the dash-dash curve. The values measured by Hall *et al.* (Ref. 16) at 29.2 eV (circles) are given for comparison. Representative error bars are shown. The solid curves are the results of calculations at 30-eV impact energy utilizing the Born-Opperheimer (BO) approximation (Ref. 35) and the Ochkur-Rudge [OR (C) and OR (STL)] approximations (Refs. 22 and 35, respectively).

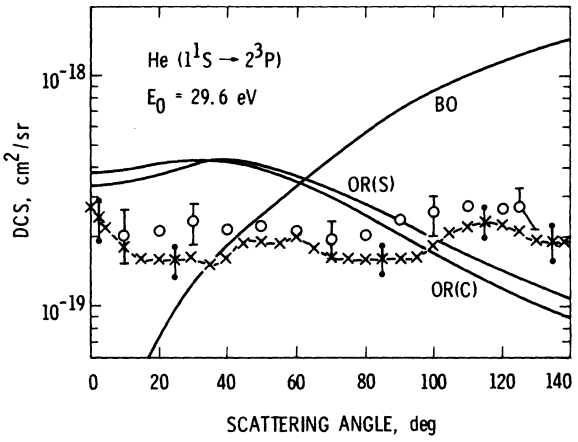

FIG. 10. Same as Fig. 9, except the cross sections are for the excitation of the $2\,^3P$ state. The calculated curves OR(C) and OR(S) are from Refs. 41 and 42, respectively.

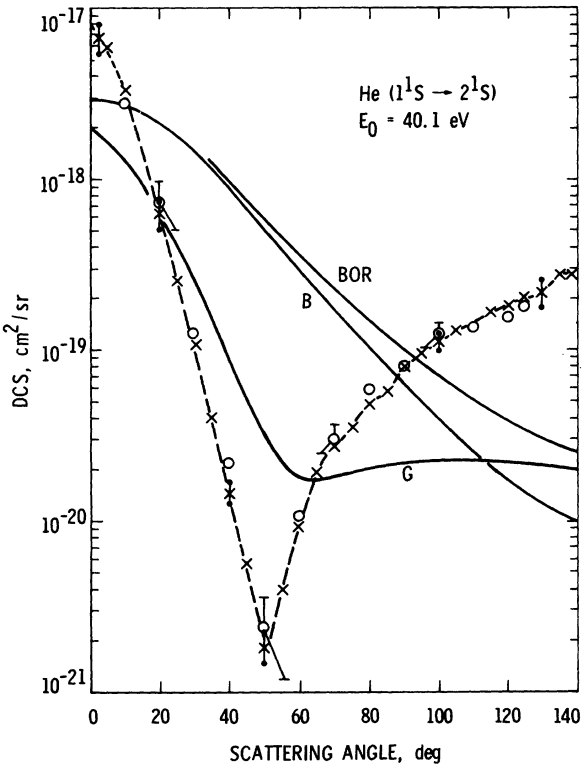

FIG. 11. Differential cross sections for the excitation of the $2\,^1S$ state. The present experimental points at 40.1 eV (crosses) are joined by the dash-dash curve. The values measured by Hall *et al.* (Ref. 16) at 39.2 eV (circles) are given for comparison. Representative error bars are shown. The solid curves are the results of calculations utilizing the Born (B), Born-Ochkur-Rudge (BOR) (Ref. 27), and Glauber (G) (Ref. 34) approximations at 40, 40, and 40.1 eV, respectively.

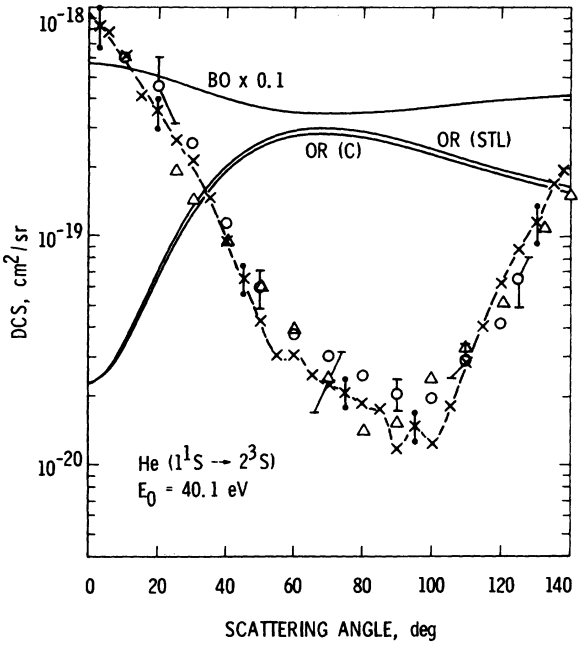

FIG. 12. Differential cross sections for the excitation of the $2\,^3S$ state. The present experimental points at 40.1 eV (crosses) are joined by the dash-dash curve. The values measured by Hall *et al.* (Ref. 16) at 39.2 eV (circles) and by Crooks *et al.* (Ref. 17) at 40 eV (triangles) are given for comparison. Representative error bars are shown. The solid curves are the results of calculations at 40-eV impact energy utilizing the Born-Opperheimer (BO) approximation (Ref. 35) and the Ochkur-Rudge [OR(C) and OR(STL)] approximations (Refs. 22 and 35, respectively).

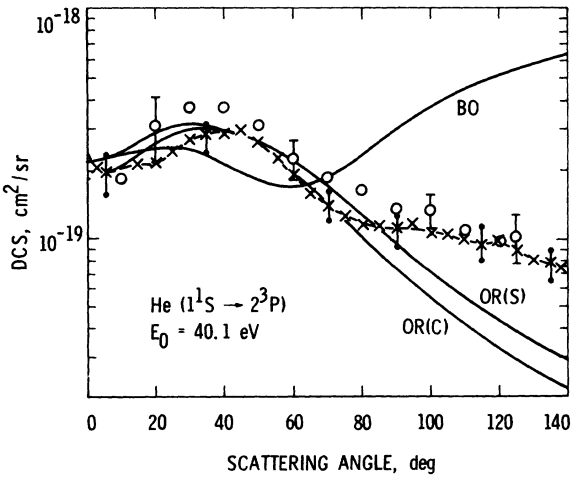

FIG. 13. Same as Fig. 12, except the cross sections are for the excitation of the $2\,^3P$ state. The curves BO and OR(S) are from Ref. 42 and the one marked as OR(C) is from Ref. 41.

function of Green *et al.*[39] for the ground state and the wave function of Morse *et al.*[40] for the $2\,^3S$ state. The calculations[41,42] for excitation of the $2\,^3P$ state using the BO and OR theories were also performed by the methods described in Refs. 22 and 23. These calculations used the wave functions of Green *et al.*[39] (for Ref. 41) and of Hylleraas[43] (for Ref. 42) for the ground state and the wave function of Morse *et al.*[40] (for Ref. 41) and of Eckart[44] (for Ref. 42) for the $2\,^3P$ state.

V. INTEGRAL CROSS SECTIONS

The experimentally determined differential cross sections have been extrapolated from 3° to 0° and from 138° to 180° and integrated over all angles. The resulting integral cross sections are summarized in Table V together with other experimental integral cross sections and also those obtained from the calculations utilizing the different plane-wave approximations.

VI. ESTIMATION OF ERRORS

The error in the ratio curves is estimated to be ±5% except at and below angles of 10°, where it is ±10%. This estimation is based on the statistical errors associated with the data points and on the reproducibility of the data points as measured at different times and under different experimental conditions. Errors due to energy dependence of the detector efficiency over the energy-loss region in question are negligible. Other types of errors that normally influence angular distribution measurements of individual excitation processes cancel out in the ratio measurements.

The errors in the DCS are the combined errors of the ratio measurements and of the $2\,^1P$ DCS, see Table VI. The errors associated with the DCS ($2\,^1P$) are of two types: About half of the error affects the absolute magnitudes of the DCS curves, but is independent of scattering angle (normalization error); the other half of the error influ-

TABLE I. Scattering intensity ratios (to $2\,^1P$) at 29.6- and 40.1-eV impact energies. The numbers in parentheses are extrapolated values.

	$E_0 = 29.6$ eV			$E_0 = 40.1$ eV		
θ (deg.)	$2\,^1S$	$2\,^3S$	$2\,^3P$	$2\,^1S$	$2\,^3S$	$2\,^3P$
0	(0.62)	(0.10)	(0.039)	(0.31)	(0.040)	(0.010)
3	0.62	•••	0.0375	0.28	0.037	0.0090
5	0.60	0.10	0.0355	0.265	0.036	0.0093
10	0.54	0.105	0.038	0.22	0.042	0.014
15	0.45	0.115	0.048	0.175	0.055	0.027
20	0.35	0.13	0.069	0.135	0.078	0.048
25	0.27	0.15	0.099	0.098	0.105	0.096
30	0.20	0.165	0.155	0.067	0.135	0.175
35	0.11	0.215	0.245	0.043	0.16	0.315
40	0.050	0.275	0.40	0.026	0.17	0.52
45	0.023	0.40	0.68	0.0145	0.175	0.79
50	0.025	0.56	1.00	0.0065	0.165	1.01
55	0.080	0.89	1.26	0.019	0.15	1.15
60	0.15	1.20	1.82	0.057	0.195	1.20
65	0.18	1.35	1.93	0.14	0.195	1.23
70	0.23	1.43	1.97	0.23	0.20	1.26
75	0.36	1.95	2.10	0.34	0.20	1.28
80	0.50	2.20	2.21	0.52	0.21	1.32
85	0.62	1.75	2.35	0.66	0.21	1.37
90	0.80	1.60	2.45	1.00	0.16	1.46
95	1.00	1.60	2.55	1.30	0.205	1.60
100	1.50	1.75	2.90	1.60	0.185	1.58
105	1.70	1.32	3.30	1.90	0.275	1.61
110	2.40	1.34	3.60	2.23	0.44	1.60
115	2.85	1.02	3.80	2.60	0.66	1.58
120	3.30	0.97	3.60	2.95	1.06	1.63
125	3.45	1.03	3.30	3.30	1.48	1.52
130	3.75	1.28	2.95	3.45	1.90	1.38
135	4.60	1.80	2.90	4.41	2.80	1.29
138	5.30	2.45	2.90	4.30	3.15	1.20

ences the angular behavior. For this reason the angular behavior of the DCS is somewhat more reliable than their absolute values.

In estimating the errors in the integral cross sections, the error associated with the extrapolation of the DCS to 0° and to 180° have been considered in addition to those associated with the DCS themselves. The estimated errors are summarized in Table VII.

In calculating the $2\,^1S$, $2\,^3S$, and $2\,^3P$ DCS from the scattering intensity ratios, a small additional error is introduced to those already listed in Table VI at angular regions where the angular behavior of the DCS in question deviates strongly from that of the $2\,^1P$ DCS. This occurs because the "effective path-length" corrections in such cases do not cancel precisely and the intensity ratios are not strictly equal to the cross-section ratios. At the present time this error cannot be estimated reliably, but on the basis of preliminary calculations[45] it is estimated to be of the order of only a few percent for the most extreme case of the cross sections considered here.

VII. DISCUSSION

In the present work the normalization was based on the $2\,^1P$ cross sections[5] (which, in turn, were

TABLE II. Experimental and theoretical cross sections for the excitation of the $2\,^1S$ state. The approximations used in the calculations are Born (B), Born-Ochkur-Rudge (BOR), and Glauber (G). The impact energies are given in the headings. The numbers in parentheses are extrapolated values.

	DCS (10^{-19} cm^2/sr)							
θ (deg.)	Expt.[a] 29.6 eV	B[b] 30 eV	BOR[b] 30 eV	G[c] 29.6 eV	Expt.[a] 40.1 eV	B[b] 40 eV	BOR[b] 40 eV	G[c] 40.1 eV
0	(42.7)	19.23	20.83	•••	(72.9)	29.40	29.96	•••
3	39.9	19.12	20.74	•••	62.2	29.12	29.68	•••
5	36.4	18.98	20.60	5.24	47.7	28.84	29.12	17.03
10	25.6	18.28	19.96	4.65	32.3	27.13	27.55	13.84
15	14.8	17.19	18.92	3.84	13.6	24.46	25.05	10.13
20	8.14	15.76	17.63	2.97	5.94	21.22	21.75	6.87
25	4.27	14.14	16.07	2.17	2.41	17.55	18.20	4.41
30	2.09	12.43	14.39	1.51	1.03	14.28	14.95	2.70
35	0.68	10.72	12.71	1.01	0.39	11.15	12.00	1.60
40	0.204	9.10	11.08	0.648	0.14	8.70	9.45	0.927
45	0.065	7.61	9.60	0.403	0.053	6.60	7.40	0.535
50	0.048	6.35	8.28	0.247	0.017	5.01	5.72	0.323
55	0.12	5.26	7.11	0.154	0.037	3.80	4.42	0.219
60	0.16	4.34	6.13	0.105	0.087	2.91	3.52	0.177
65	0.17	3.58	5.29	0.084	0.182	2.13	2.80	0.169
70	0.19	2.96	4.65	0.080	0.26	1.71	2.25	0.176
75	0.28	2.47	3.97	0.086	0.33	1.31	1.81	0.188
80	0.36	2.06	3.47	0.096	0.46	1.01	1.47	0.200
85	0.43	1.72	3.05	0.108	0.54	0.78	1.20	0.210
90	0.53	1.45	2.69	0.120	0.75	0.61	0.99	0.217
95	0.64	1.22	2.38	0.131	0.92	0.48	0.82	0.221
100	0.95	1.04	2.12	0.140	1.06	0.38	0.69	0.222
105	1.06	0.89	1.90	0.147	1.22	0.31	0.59	0.221
110	1.48	0.76	1.71	0.153	1.38	0.25	0.50	0.218
115	1.77	0.66	1.54	0.157	1.57	0.21	0.43	0.215
120	2.09	0.56	1.40	0.160	1.74	0.17	0.38	0.210
125	2.21	0.51	1.29	0.162	1.91	0.14	0.34	0.206
130	2.44	0.45	1.19	0.163	2.04	0.12	0.30	0.201
135	3.04	0.41	1.10	0.163	2.63	0.11	0.27	0.196
138	3.51	•••	•••	•••	2.63	•••	•••	•••
140	(3.9)	0.37	1.03	0.163	(2.7)	0.096	0.25	0.192
160	(8.6)	0.28	0.85	•••	(2.7)	0.067	0.20	•••
180	(12.5)	0.26	0.80	•••	(2.7)	0.060	0.18	•••

[a] Present work. [b] Reference 27. [c] Reference 34.

normalized to the excitation functions of Donaldson *et al.*[46]). The excellent agreement both in magnitude and in over-all angular behavior between the present results and those of Hall *et al.*[16] and Crooks *et al.*[17] establishes the reliability of the experimental cross sections at these two energies and makes them ideally suited for checking new electron scattering instruments. The agreement is especially significant since the normalizations were carried out by completely different and independent methods. The $2\,^1P$ DCS curves were found to be smoothly varying functions of scattering angle.[5] The well-defined structure in the $I(2\,^3S)/I(2\,^1P)$ curve must, therefore, be associated with the $2\,^3S$ DCS curves. There is some indication for structure in the $2\,^1S$ and $2\,^3P$ DCS curves also. In these cases, however, the structure is comparable to the experimental errors and one cannot be as certain as in the $2\,^3S$ case. (The error bars associated with the cross-section values represent the total error. A significant part of it is calibration error, which shifts the whole curve but does not affect the shape.)

The DCS curves for the optically forbidden transitions are quite complex and constitute a very severe test for theoretical models. At the present time no practical calculational methods exist which would properly predict differential cross sections over a wide angular range for these optically forbidden transitions at intermediate impact energies. It is clear that plane-wave approximations, even though they sometimes predict

TABLE III. Experimental and theoretical cross sections for the excitation of the $2\,^3S$ state. The approximations used in the calculations are Born-Opperheimer (BO) and Ochkur-Rudge (OR). The impact energies are indicated in the headings. The numbers in parenthesis are extrapolated values.

	DCS (10^{-19} cm^2/sr)					
θ (deg.)	Expt.[a] 29.6 eV	BO[b] 30 eV	OR[b] 30 eV	Expt.[a] 40.1 eV	BO[b] 40 eV	OR[b] 40 eV
0	(7.57)	125.1	0.646	(9.39)	56.5	0.225
3	...	124.8	0.658	8.22	56.4	0.234
5	6.25	124.6	0.674	7.15	56.0	0.251
10	4.98	123.2	0.753	6.17	54.8	0.330
15	3.80	121.2	0.887	4.25	52.6	0.478
20	3.02	118.4	1.08	3.43	50.1	0.697
25	2.38	115.0	1.33	2.64	47.6	0.988
30	1.72	111.7	1.62	2.10	44.8	1.33
35	1.34	108.0	1.95	1.44	42.2	1.70
40	1.12	104.7	2.30	0.94	40.3	2.06
45	1.13	101.3	2.65	0.64	38.3	2.38
50	1.08	98.5	2.99	0.42	36.9	2.65
55	1.32	96.0	3.30	0.30	36.1	2.84
60	1.32	93.8	3.55	0.30	35.5	2.96
65	1.26	92.1	3.78	0.25	35.2	3.02
70	1.18	90.7	3.94	0.22	35.0	3.07
75	1.49	89.8	4.08	0.20	35.2	2.99
80	1.58	89.0	4.14	0.18	35.5	2.91
85	1.21	88.4	4.17	0.17	35.8	2.80
90	1.05	88.2	4.17	0.12	36.4	2.69
95	1.03	88.2	4.14	0.14	36.9	2.56
100	1.11	88.4	4.11	0.12	37.8	2.44
105	0.82	88.7	4.03	0.18	38.3	2.31
110	0.82	89.0	3.97	0.27	39.2	2.19
115	0.63	89.3	3.89	0.40	39.7	2.08
120	0.61	89.8	3.80	0.62	40.3	1.97
125	0.66	90.1	3.69	0.86	40.8	1.88
130	0.83	90.7	3.61	1.12	41.7	1.79
135	1.19	91.2	3.55	1.68	42.0	1.72
138	1.62	...	...	1.94	...	...
140	(1.9)	91.8	3.47	(2.1)	42.5	1.65
160	(4.4)	93.2	3.24	(3.1)	43.9	1.47
180	(6.1)	93.5	3.19	(3.8)	44.5	1.41

[a] Present work.

[b] Reference 35.

cross sections of the right order of magnitude, are unable to predict the proper angular distributions. The Glauber approximation gives much better agreement than the plane-wave models with the experimental data for the $2\,^1S$ excitation. It is evident, however, from Figs. 5 and 8 that the finer details and the high-angle behavior of the cross-section curves are not accurately described by this approximation either. The high-angle behavior might be improved by somehow including exchange in this model. Calculations for the $2\,^3S$ and $2\,^3P$ excitations by the distorted-wave method are presently being carried out.[47] The indications are that there is an agreement between the calculated and the experimental DCS curves considering the over-all shape and magnitude, but there are deviations at high scattering angles and fine details of the experimental curves are not predicted by the calculations. Very recently Csanak *et al.*[48] formulated a many-body Green's-function method for inelastic electron He scattering, but numerical calculations have not yet been carried out.

The integral cross sections calculated by the different first-order plane-wave models are, with the exception of the BO model for the $2\,^3S$ excitation, all the same order of magnitude as the experimental results. It has been well known[49,50] that the BO approximation gives much poorer results for S-S than for S-P transitions. The present results support this observation. The integral cross sections calculated by Van den

TABLE IV. Experimental and theoretical cross sections for the excitation of the $2\,^3P$ state. The approximations used in the calculations are Born-Opperheimer (BO) and Ochkur-Rudge (OR). The impact energies are indicated in the headings. The numbers in parentheses are extrapolated values.

	DCS (10^{-19} cm^2/sr)					
θ (deg.)	Expt.[a] 29.6 eV	BO[b] 30 eV	OR[b] 30 eV	Expt.[a] 40.1 eV	BO[b] 40 eV	OR[b] 40 eV
0	(2.68)	0.19	3.36	(2.35)	2.24	1.86
3	2.41	0.21	3.36	2.00	2.25	1.90
5	2.16	0.23	3.38	1.85	2.27	1.93
10	1.80	0.34	3.47	2.06	2.34	2.12
15	1.59	0.51	3.61	2.08	2.43	2.38
20	1.60	0.73	3.78	2.11	2.50	2.65
25	1.56	0.98	3.94	2.37	2.50	2.88
30	1.62	1.25	4.08	2.68	2.44	3.02
35	1.52	1.54	4.17	2.80	2.30	3.08
40	1.63	1.84	4.17	2.86	2.13	3.02
45	1.92	2.16	4.14	2.93	1.96	2.88
50	1.93	2.52	4.06	2.59	1.80	2.67
55	1.87	2.91	3.89	2.25	1.71	2.43
60	2.00	3.36	3.72	1.86	1.68	2.17
65	1.81	3.86	3.50	1.57	1.73	1.92
70	1.62	4.42	3.27	1.39	1.86	1.68
75	1.61	5.04	3.02	1.27	2.04	1.46
80	1.59	5.71	2.80	1.16	2.33	1.26
85	1.62	6.44	2.58	1.12	2.65	1.09
90	1.62	7.19	2.36	1.09	2.99	0.94
95	1.64	7.98	2.16	1.14	3.36	0.81
100	1.83	8.70	1.98	1.05	3.75	0.71
105	2.05	9.54	1.82	1.04	4.14	0.62
110	2.20	10.33	1.67	1.00	4.53	0.54
115	2.37	11.11	1.54	0.96	4.90	0.48
120	2.28	11.84	1.42	0.97	5.23	0.43
125	2.12	12.54	1.32	0.88	5.57	0.38
130	1.93	13.21	1.23	0.82	5.88	0.34
135	1.92	13.83	1.16	0.77	6.16	0.31
138	1.92	...	...	0.74	...	...
140	(1.9)	14.39	1.09	(0.73)	6.41	0.29
160	(2.0)	15.98	0.92	(0.71)	7.14	0.23
180	(2.1)	16.54	0.87	(0.84)	7.39	0.21

[a] Present work.

[b] Reference 42.

TABLE V. Integral cross sections.

State	Method	E_0 (eV)	$Q(10^{-19}$ cm$^2)$	E_0 (eV)	$Q(10^{-19}$ cm$^2)$
$2\,^1S$	Present expt.	29.6	29.1 ±7.0	40.1	21.1 ±4.0
	Hall *et al.*[a] expt.	29.2	24.1 ±7.0	39.2	21.0 ±6
	Calc. B[b]	30	42.56	40	39.20
	Calc. BOR[b]	30	58.80	40	44.24
	Calc. VDB[c]	30	28.84	40	26.60
$2\,^3S$	Present expt.	29.6	19.4 ±4.5	40.1	12.2 ±2.4
	Hall *et al.*[a] expt.	29.2	17.0 ±5.0	39.2	14.0 ±12.0
	CDGR[d] expt.	...	...	40	10.3 ±3.1
	Calc. BO[e]	30	1181.6	40	496.2
	Calc. OR[e]	30	43.46	40	27.88
$2\,^3P$[f]	Present expt.	29.6	23.4 ±4.2		17.7 ±3.2
	Hall *et al.*[a] expt.	29.2	27.6 ±5.4		21.4 ±4.2
	Jobe-St. John[g]	30	21	40	15.5
	Calc. BO[h]	30	96.60		46.20
	Calc. OR[h]	30	31.36		16.13

[a] Reference 16.
[b] Reference 27.
[c] Van den Bos, Ref. 51.
[d] Crooks, Du Bois, Golden, and Rudd, Ref. 17.
[e] Reference 35.
[f] Previous calculations on the $2\,^3P$ integral cross sections {Massey and Moiseiwitsch, Proc. Roy. Soc. A258, 147 (1960); Ochkur and Brattsev, Opt. Spectrosk. 19, 490 (1965) [Opt. Spectrosc. 19, 274 (1965)]; Lashmore-Davis, Proc. Phys. Soc. 86, 783 (1965); Bell, Eisso, and Moiseiwitsch, Proc. Roy. Soc. 88, 57 (1966); Ojha, Tiwari, and Rai, J. Phys. B 5, 2231 (1972)} all gave values of the same order of magnitude as the present theoretical results.
[g] J. D. Jobe and R. M. S. St. John, Phys. Rev. 164, 117 (1967).
[h] Reference 42.

Bos[51] for the $2\,^1S$ excitation are in the best agreement with experiment. The calculation was carried out in the B approximation using less accurate wave functions than the ones used to obtain the present results.[27] The better agreement with experiment must therefore be fortuitous.

It would be interesting and important to apply more refined models to the optically forbidden transitions of the $n=2$ manifold and one purpose of this paper is to give experimental data for testing these models. A partial wave analysis of the experimental data would be[35,52] very useful in checking the theoretical models and approximations.

TABLE VI. Estimation of errors associated with the differential cross sections at 29.6 and 40.1 eV.

Source of error	Estimated error (%) Angular range		
	3°–10°	10°–90°	90°–138°
Error in the DCS (X)/DCS ($2\,^1P$)[a]	10	5(10)[b]	5
RMS error in DCS ($2\,^1P$)[c]	18	15	18
Total error in DCS (X)[d]	20	14(18)[b]	18

[a] X refers to $2\,^1S$, $2\,^3S$, or $2\,^3P$.
[b] The number in parentheses refers to the $2\,^1S$ cross sections in the 40°–60° angular range. The larger error in this range is due to the very small value of the scattering intensity associated with the $2\,^1S$ excitation.
[c] Reference 5.
[d] The total error is the square root of the sum of the squares of the component errors.

TABLE VII. Estimates of errors associated with the integral cross section.

Source of error	Estimated error (%) 29.6 eV $2\,^1S$	$2\,^3S$	$2\,^3P$	40.1 eV $2\,^1S$	$2\,^3S$	$2\,^3P$
Total error in DCS (X) [a]	18	18	18	18	18	18
Extrapolation error	16	14	2	5	8	2
Total error in Q [b]	24	23	18	19	20	18

[a] X refers to $2\,^1S$, $2\,^3S$, or $2\,^3P$. The values are taken from Table VI.
[b] The total error is the square root of the sum of the squares of the component errors.

ACKNOWLEDGMENTS

I would like to express my thanks to D. C. Cartwright (Aerospace Corp.), J. C. Steelhammer (University of Minnesota and Oak Ridge National Laboratory), S. Lipsky and D. G. Truhlar (University of Minnesota), and A. C. Yates and A. Tenney (Indiana University) for carrying out calculations for comparison with the present experimental measurements; to R. I. Hall, G. Joyez, M. Mazeau, J. Reinhardt, and C. Schermann (University of Paris) for giving to me the results of their measurements before they appeared in publication; to G. B. Crooks, R. C. Du Bois, D. E. Golden, and M. E. Rudd (University of Nebraska) for sending me their $2\,^3S$ results in tabular form; and to A. Chutjian and W. Williams (Jet Propulsion Laboratory) for their comments and help concerning the measurements. The many valuable discussions with D. G. Truhlar and his critical reading of the manuscript are greatly appreciated.

*Paper presents the results of one phase of research carried out at the Jet Propulsion Laboratory, California Institute of Technology, under Contract No. NAS7-100 sponsored by the National Aeronautics and Space Administration.

[1]H. W. S. Massey and E. H. S. Burhop, *Electronic and Ionic Impact Phenomena*, 2nd ed. (Clarendon, Oxford, 1969), Vol. I.
[2]D. G. Truhlar, J. K. Rice, A. Kuppermann, S. Trajmar, and D. C. Cartwright, Phys. Rev. A **1**, 778 (1970).
[3]D. G. Truhlar, J. K. Rice, S. Trajmar, and D. C. Cartwright, Chem. Phys. Lett. **9**, 299 (1971).
[4]D. H. Madison and W. N. Shelton, Phys. Rev. A 7, 499 (1973).
[5]D. G. Truhlar, S. Trajmar, W. Williams, S. Ormonde, and B. Torres (unpublished).
[6]G. E. Chamberlain, H. G. M. Heidemann, J. Arol Simpson, and C. E. Kuyatt, in *Abstracts of Papers of the Fourth International Conference on the Physics for Electronic and Atomic Collisions* (Science Bookcrafters, Hastings-on-Hudson, N.Y., 1965), p. 378.
[7]J. Arol Simpson, M. G. Menendez, and S. R. Mielczarek, Phys. Rev. **150**, 76 (1966).
[8]E. N. Lassettre, A. Skerbele, M. A. Dillon, and K. J. Ross, J. Chem. Phys. **48**, 5066 (1968).
[9]J. K. Rice, A. Kuppermann, and S. Trajmar, J. Chem. Phys. **48**, 945 (1968).
[10]A. Kuppermann, J. K. Rice, and S. Trajmar, J. Chem. Phys. **72**, 3894 (1968).
[11]S. Trajmar, J. K. Rice, and A. Kuppermann, Adv. Chem. Phys. 18, 15 (1970).
[12]R. I. Hall, G. Joyez, J. Mazeau, J. Reinhardt, and C. Schermann, C.R. Acad. Sci. (Paris) **272**, 743 (1971).
[13]J. K. Rice, D. G. Truhlar, D. C. Cartwright, and S. Trajmar, Phys. Rev. A **5**, 762 (1972).
[14]C. B. Opal and E. C. Beaty, J. Phys. B **5**, 627 (1972).
[15]C. B. Crooks, Ph.D. thesis (University of Nebraska, Lincoln, Ne, 1972) (unpublished).
[16]R. I. Hall, G. Joyez, J. Mazeau, J. Reinhardt, and C. Schermann (unpublished).
[17]G. B. Crooks, R. D. DuBois, D. E. Golden, and M. E. Rudd, Phys. Rev. Lett. **29**, 327 (1972).
[18]A. C. Yates and A. Tenney, Phys. Rev. A **6**, 1451 (1972).
[19]G. E. Chamberlain, S. R. Mielczarek, and C. E. Kuyatt, Phys. Rev. A **2**, 1905 (1970).
[20]M. B. Hidalgo and S. Geltman, J. Phys. B **5**, 617 (1972).
[21]D. A. Kohl, D. P. Duncan, F. H. Tuley, and M. Fink, J. Chem. Phys. **56**, 3769 (1972).
[22]D. C. Cartwright, Ph.D. thesis (California Institute of Technology, Pasadena, Calif., 1968) (unpublished). An error in the DCS for excitation of the $2\,^3P$ state has been corrected.
[23]J. C. Steelhammer, Ph.D. thesis (University of Minnesota, Minneapolis, Minn., 1971) (unpublished).
[24]L. Vriens, J. Arol Simpson, and S. R. Mielczarek, Phys. Rev. **165**, 7 (1968).
[25]A. Chutjian, D. C. Cartwright, and S. Trajmar, Phys. Rev. Lett. (to be published).
[26]D. Andrick and A. Bitsch (unpublished).
[27]D. G. Truhlar (private communication).
[28]H. Bethe, Ann. Phys. (Leipz.) **5**, 325 (1930).
[29]D. G. Truhlar, D. C. Cartwright, and A. Kuppermann, Phys. Rev. **175**, 113 (1968).
[30]K. L. Bell, D. J. Kennedy, and A. E. Kingston, J. Phys. B **1**, 204 (1968).
[31]D. G. Truhlar, Ph.D. thesis (California Institute of Technology, Pasadena, Calif., 1969) (unpublished).
[32]A. W. Weiss, J. Res. Natl. Bur. Stand. (U.S.) **71A**, 163 (1967).
[33]Y. -K. Kim and M. Inokuti, Phys. Rev. **175**, 176 (1968).
[34]A. C. Yates and A. Tenney (private communication).
[35]J. C. Steelhammer, D. G. Truhlar, and S. Lipsky (private communication).
[36]J. R. Oppenheimer, Phys. Rev. **32**, 361 (1928).

[37]D. R. Bates, A. Fundaminsky, J. W. Leech, and H. S. W. Massey, Philos. Trans. R. Soc. Lond. **243**, 93 (1950).
[38]M. R. H. Rudge, Proc. Phys. Soc. Lond. **85**, 607 (1965); Proc. Phys. Soc. Lond. **86**, 763 (1965).
[39]L. C. Green, M. M. Mulder, M. N. Lewis, and J. W. Woll, Phys. Rev. **93**, 757 (1954).
[40]P. M. Morse, L. A. Young, and E. S. Haurwitz, Phys. Rev. **48**, 948 (1935).
[41]D. C. Cartwright (private communication).
[42]J. C. Steelhammer (private communication).
[43]E. A. Hylleraas, Z. Phys. **54**, 347 (1929).
[44]C. Eckart, Phys. Rev. **36**, 878 (1930).
[45]R. T. Brinkmann and S. Trajmar (unpublished).
[46]F. G. Donaldson, M. A. Hender, and J. W. McConkey, J. Phys. B **5**, 1192 (1972).
[47]W. N. Shelton (private communication).
[48]Gy. Csanak, H. S. Taylor, and D. N. Tripathy, Bull. Am. Phys. Soc. **17**, 1134 (1972).
[49]B. L. Moiseiwitsch and S. J. Smith, Rev. Mod. Phys. **40**, 238 (1968).
[50]D. G. Truhlar, D. C. Cartwright, and A. Kuppermann, Phys. Rev. **175**, 113 (1968).
[51]J. Van den Bos, Physica (The Hague) **42**, 245 (1969).
[52]R. T. Poe (private communication).

PHYSICAL REVIEW A VOLUME 8, NUMBER 1 JULY 1973

Threshold Behavior of Inelastic-Scattering Cross Sections*

J. N. Bardsley† and R. K. Nesbet
IBM Research Laboratory, San Jose, California 95193
(Received 12 March 1973)

The behavior of scattering cross sections near an excitation threshold is examined for the case of long-range potentials. The theory is confirmed by computations of e-Li scattering. Recent observations of threshold structure in e-Na collisions are ascribed to a ^1D resonance of Na^-. A true cusp should occur only in the ^1P partial cross section.

The effects of long-range potentials on the threshold behavior of elastic-scattering cross sections were studied some time ago, principally by O'Malley, Spruch, and Rosenberg[1] and by Levy and Keller.[2] However, there has been little analysis of the effects of such potentials on inelastic collisions. The purpose of this paper is to extend the analysis of Levy and Keller[2] to inelastic scattering, and to relate the results to recent experiments involving alkali atoms. One particular feature that we will examine is the appearance of Wigner cusps at excitation thresholds. Our analysis will be applicable to any atom except hydrogen, for which special problems arise owing to the l degeneracy. These special problems have been studied by Gailitis and Damburg[3] and others.

The analysis of Levy and Keller[2] is based on the variable-phase method, which has been extended to multichannel problems by several authors.[4,5] For each channel α, the associated single-particle function $\phi_{\alpha\beta}(r)$ is written

$$\phi_{\alpha\beta}(r) = w_{0\alpha}(r)\delta_{\alpha\beta} + w_{1\alpha}(r)t_{\alpha\beta}(r). \tag{1}$$

The index β denotes the incident channel; $w_{0\alpha}(r)$ and $w_{1\alpha}(r)$ are independent functions which have the asymptotic form appropriate for the channel α. If there is no unscreened Coulomb interaction in the asymptotic region, these can be expressed in terms of spherical Bessel functions. For open channels we take

$$w_{0\alpha}(r) = k_\alpha^{1/2} r j_{l_\alpha}(k_\alpha r), \tag{2}$$

$$w_{1\alpha}(r) = -k_\alpha^{1/2} r n_{l_\alpha}(k_\alpha r). \tag{3}$$

The scattering information is contained in the matrix $t_{\alpha\beta}(r)$. The limit of $t_{\alpha\beta}(r)$, as $r \to \infty$, is the reactance matrix $K_{\alpha\beta}$, whose eigenvalues are the tangents of the eigenphases.

By substitution in the Schrödinger equation we obtain an integral equation for $t_{\alpha\beta}(r)$ of the form[4]

$$t_{\alpha\beta}(r) = -2\int_0^r \sum_\gamma \sum_\delta [\delta_{\alpha\gamma} w_{0\gamma}(r') + t_{\alpha\gamma}(r') w_{1\gamma}(r')] \times V_{\gamma\delta}(r')[w_{0\delta}(r')\delta_{\delta\beta} + w_{1\delta} t_{\delta\beta}(r')]\, dr', \tag{4}$$

where $V_{\gamma\delta}(r)$ is the interaction potential, expressed in matrix form. The K-matrix Born approximation[6] can be obtained by neglecting the terms involving $t(r')$ on the right-hand side of Eq. (4). Substituting for $w_{0\beta}(r)$, we obtain

$$K_{\alpha\beta} \equiv t_{\alpha\beta}(\infty) = -k_\alpha^{1/2} k_\beta^{1/2} \int_0^\infty 2 V_{\alpha\beta}(r) j_{l_\alpha}(k_\alpha r) j_{l_\beta}(k_\beta r) r^2 dr. \tag{5}$$

As shown for single-channel scattering by Levy and Keller,[2] the dominant term in the threshold behavior is given by Eq. (5).

Let us suppose that we have one or more old channels labeled $\alpha, \beta, \ldots$, and one or more new